Efficiency of Steel and Macro-Synthetic Structural Fibers on the Flexure-Shear Behaviour of Prestressed Concrete Beams

Suhas S Joshi[1], Nikesh Thammishetti[2], Suriya Prakash S[3*]

[1]Graduate student, Email id: ce16mtech01001@iith.ac.in
[2]PhD candidate, Email id: ce16resch11005@iith.ac.in
[3*]Associate Professor and Corresponding Author, Email id: suriyap@iith.ac.in

[1, 2, 3] Department of Civil Engineering, Indian Institute of Technology Hyderabad, India.

Abstract

The efficiency of steel and structural synthetic fibers on the performance improvement of prestressed concrete (PSC) beams under combined flexure-shear is studied. Results of eleven PSC beams tested at a shear span (a) to depth (d) ratio of five are presented. Discrete steel and macro synthetic structural polyolefin fibers of varying dosages of 0.35%, 0.7% and 1.0% by volume of concrete were used. The effect of fiber addition on overall load – displacement, load-strain, and strain energy absorption capacity of PSC beams is analysed. Other parameters such as shear span to depth ratio (a/d), compressive strength of concrete, prestressing reinforcement ratio were kept constant. The test results portray that the addition of steel fibers stiffens the post cracking response, increases the strain energy absorption capacity more efficiently when compared to macro synthetic fibers (Polyolefin). The failure mode changed from less ductile flexure-shear to more ductile flexure dominant mode at 0.35% and 0.70% volumetric dosage of steel and synthetic fibers, respectively. The strain energy absorption capacity increased by more than 100% at 1.0% fiber addition for both steel and macro-synthetic fibers.

Keywords: Ductility; Synthetic fibers; Prestressed Concrete Beam; Steel fibers.

1. INTRODUCTION

Fiber Reinforced Concrete (FRC) is tailored by addition of randomly oriented fibers to plain concrete. FRC has gained popularity in the recent years due to advantages like (i) ease of availability of fibers; (ii) better performance in serviceability regime; and (iii) improved mechanical properties in compression, tension, flexure, and shear when compared to the conventional concrete [1-5]. Apart from crack resistance, steel fibers can also be used to replace the conventional transverse reinforcement in the concrete [6,7]. Though steel fibers have superior mechanical properties compared to that of synthetic fibers, they decrease the workability and creates balling effect at higher dosage. On the other hand, structural synthetic fibers, being non-corrosive and malleable, have gained attention in the recent years. They are also used for reinforcing cementitious materials to control the crack propagation and improve the overall structural performance [8,9]. Polyolefin fibers comes under the category of synthetic fibers. Polyolefin fibers are categorized as micro-synthetic and macro-synthetic (structural) fibers. Micro-synthetic fibers are typically 12 mm long and 0.018 mm in diameter, whereas the macro ones are significantly larger with 40-50 mm in length and 0.3-1.5 mm in diameter.

Number of previous work have focused on the behaviour of fiber reinforced concrete under flexure and shear loadings. Sahoo and Kumar [10] tested steel reinforced concrete beams and observed increase in deformability (ductility) and decrease in crack widths. Few researchers [11,12] have used fibers as secondary reinforcement for the concrete elements to improve the shear performance. Some works in the past have [13-15] focused on the influence of fibers on the fresh and hardened properties as well as on the shear capacity of prestressed beams. Yazdanbakhsh et al. [16] carried out analytical studies to predict the shear capacity of synthetic fiber reinforced concrete beams based on the model originally developed for steel fiber reinforcement. They noted that shear capacities from RILEM 162-TDF [17] recommendations were found to be more conservative than Fib-MC2010 [18] for synthetic fiber reinforced beams. Alhozaimy et al. [19] investigated the mechanical properties and effects of pozzolanic materials on concrete reinforced with fibrillated polypropylene fibers of low volume fractions (< 0.3%). They reported that fiber content variation has no significant effect on the compressive and flexural strength of FRC but improved its toughness and impact resistance.

Thomas and Ramaswamy [20] noted that addition of fibers reduced the crack width of prestressed concrete beams. Harajli [21] noted that the presence of fibers enhanced the bond strength of rebars and reduced its bond degradation. Sahoo and Sharma [22] observed that flexural capacity did not improve significantly when more than 0.5% by volume of steel fibers were added to reinforced concrete beams with and without stirrups. Tiberti et al. [23] presented dependency of crack propagation on the concrete strength of steel fiber reinforced concrete (SFRC). They noted that steel fibers are more effective when used in high strength concrete (HSC) than in normal strength concrete (NSC). Ramzi and Omer [24] studied the flexural strength of under-reinforced and over-reinforced concrete T-beams with steel fiber. Their results indicated that presence of steel fibers improved the ultimate strength and reduced the crack width. Abbas and Khan [25] carried out pull-out tests on SFRC beams and concluded that the ultimate pull-out load depends on the fiber size and its embedment length.

Yoo et al. [26] presented the effects of strength, fiber content and strain-rate on flexural response of SFRC under quasi-static and impact loads. Banthia and Sappakittipakorn [27] investigated the toughness enhancement of SFRC through fiber hybridization. They noted that flexural toughness and deflection hardening properties were improved. To account for the post peak response of different cement based materials Fantilli et al. [28] defined a unique function. Amin et al. [29] reported the material characterisation of macro synthetic fiber reinforced concrete through a series of tension tests. The authors concluded that the degree of variability in the results is lowest in case of round panel tests compared to uniaxial tension tests. Though number of previous work have focused on fiber reinforced concrete, the effect of structural macro-synthetic fiber reinforcement on the behaviour of high strength prestressed concrete beams has not been explored adequately.

2.0 RESEARCH SIGNIFICANCE

Most of the previous studies focused on behaviour of concrete elements reinforced with steel fibers and fibrillated or micro-synthetic fibers. Inadequate information is available on the performance of structural synthetic fibers (polyolefin) on flexure, shear and flexure-shear behaviour of prestressed concrete beams and is the focus of this investigation. Thus, this study aims at the following: (i) study the effect of different dosages of steel and synthetic fibers on flexure-shear behaviour of prestressed concrete beams, and (ii) study the crack propagation, strain reduction of prestressing strand and assess the change in failure modes at different fiber additions.

3.0 EXPERIMENTAL INVESTIGATION

3.1 Test specimens

The experimental program includes casting and testing of full-scale prestressed concrete beams of rectangular cross section (200 mm x 300 mm) and length of 3500 mm. The beams were reinforced with two prestressing strands of 12.7 mm diameter corresponding to prestressing steel reinforcement ratio of 0.4%. Jacking force is applied to each of the strands to obtain an initial prestressing strain of 0.004 in accordance with IS 1343 [30]. The specimens were divided into three series: beams made of plain concrete (Control), beams made of steel fiber reinforced concrete (SF series) and beams made of polyolefin fiber reinforced concrete (PO Series). Each of the SF and PO series were further categorised based on the fiber dosage. The nomenclature details of different series used in the study are presented in Table 1.

Table 1: Details of concrete series

	Type of fiber		Dosage of fiber (%)
	Steel	Polyolefin	
	Control	Control	0.00
	SF35	PO35	0.35
Series	SF70	PO70	0.70
	SF100	PO100	1.00

Table 2: Mix Design Details

Concrete	Quantities in kg/m^3									
	Aggregate				C	F	W	HRWR	SF	PO
	20 mm	10 mm	CSS	NRS						
Control									-	-
SF35									27.47	-
SF70									54.94	-
SF100	754.0	355.0	415.0	313.0	428.0	22.0	165.0	2.5	78.50	-
PO35									-	3.18
PO70									-	6.37
PO100									-	9.10

CSS - Crushed Stone Sand, NRS - Natural River Sand, C – Cement, F – Flyash, W – Water, HRWR – High Range Water Reducing admixture, SF – Steel Fiber, PO- Polyolefin Fiber

3.2. Material Properties

Concrete mix design was developed as per IS 10262-2009 [31] with a target compressive strength of 58 MPa. Table 2 presents the mix details. Coarse aggregate blended of 10 mm and 20 mm aggregate, crushed stone sand, natural river sand, flyash and high range water reducing admixture (HRWR) were used to achieve workable concrete of 58 MPa strength. Addition of fibers inversely affected the workability of concrete mix. The compressive strength of concrete cubes and cylinders tested on 28th day is reported in **Error! Not a valid bookmark self-reference.**. The prestressing strands with seven wired low relaxation steel (12.7 mm diameter, effective area of 99.7 mm^2) were used as reinforcement. Prestressing strands with a constant eccentricity (e) of 100 mm was used resulting in straight profile of the strands. Tensile strength and modulus of elasticity of the strands were measured to be 1860 MPa and 196.5 GPa, respectively from the coupon tests. The hooked end steel fibers and macro- synthetic polyolefin fibers were used in developing concrete mixes of SF and PO series respectively. The shapes and various properties of the fibers used are presented in Fig. 1 and Table 4 respectively.

Table 3: Compressive strength of concrete

Specimen	Average Compressive strength (MPa) [SD]		Specimen	Average Compressive strength (MPa) [SD]	
	Cube	Cylinder		Cube	Cylinder
Control	65[2.42]	43[1.85]	Control	65[2.42]	43[1.85]
SF35	62 [0.75]	47[2.40]	PO35	67[2.82]	48[2.44]
SF70	61[0.15]	47[4.21]	PO70	74[1.33]	50[4.72]
SF100	63 [0.30]	50[3.98]	PO100	72[2.05]	46[4.30]

[SD] – Standard Deviation

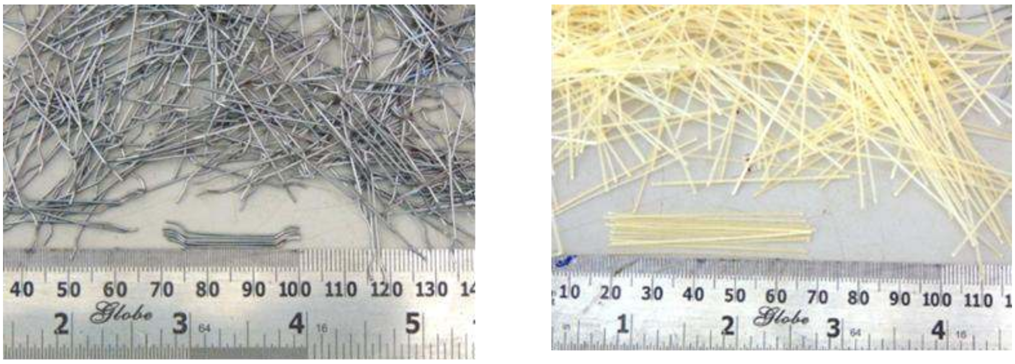

(a) (b)

Fig. 1: Fibers (a) Steel Fiber and (b) Structural Synthetic Fibers

Table 4: Properties of Steel and Polyolefin Fibers

	Fiber Type	
Properties	Steel	Polyolefin
Specific gravity	7.85	0.91
Length (mm)	30	50
Tensile strength (MPa)	1000	618
Modulus of elasticity (GPa)	200	10
Diameter (mm)	0.6	0.5
Aspect ratio	50	100

3.3 Test Setup and Instrumentation

The shear span to depth ratio (a/d) of five is considered to simulate the flexure-shear behavior. Kani [32] investigated the effect of different a/d ratios on the behaviour of RC beams. The author found that the beams had flexure dominant behaviour above a/d ratio of 6. The author also observed that the a/d ratio of 2.5 is a transition point below which the beams are shear critical and the corresponding bending moment at failure was found to be minimum. Below the a/d ratio of 2.5, the beam is shown to develop an arch action with a considerable reserve strength beyond the first cracking point. Similarly, for a/d ratio between 2.5 and 6, the failure was due to sudden diagonal shear tension and flexure-shear mode. Therefore, a higher a/d ratio of five is considered to study the influence of steel and synthetic fibers on the flexure-shear behaviour. All the beams were tested in a four-point bending configuration. The beams were simply supported on I-beams. The horizontal movement of the support is restrained. The specimens are not restrained as they are simply supported and the same is portrayed in the Figure 2. Support width is expected to have minimal influence on the behaviour as the specimens are tested at higher a/d ratio of 5. The effect of different a/d ratio, support conditions, cross section details and size effect on the behaviour of fiber reinforced prestressed concrete beams would be interesting and is scope for further work. Eleven beams were cast with different fiber dosages of 0.00%, 0.35%, 0.70% and 1.00% and were water-cured for a period of 28 days at room temperature. The beam schematic and loading configuration is presented in the Fig. 2.

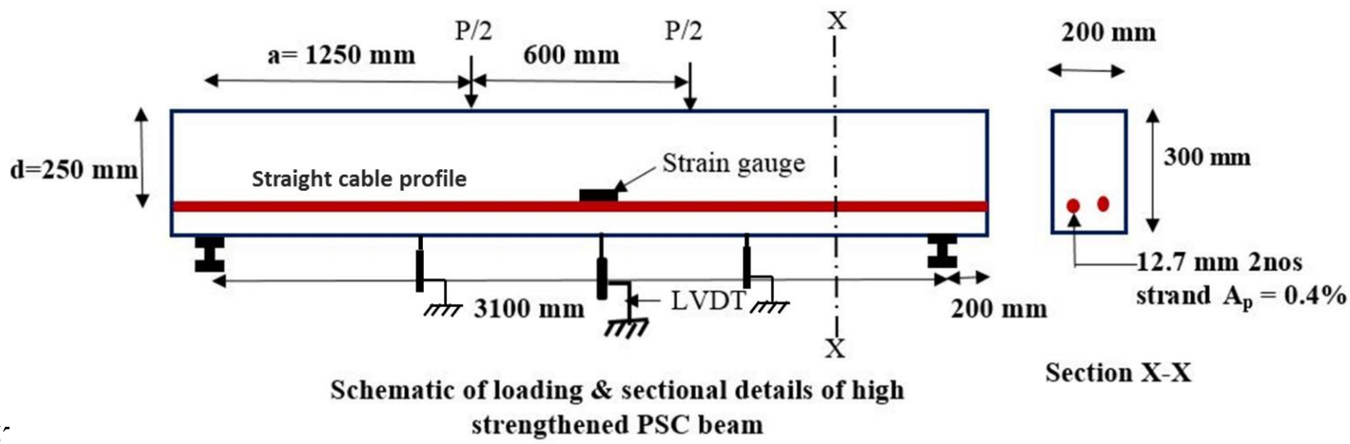

Fig. 2: Schematic Details of the Test specimen

The beams were tested using a servo controlled hydraulic MTS actuator of 250 kN capacity. Load from the actuator was transferred to the specimen through spreader beam and then to the two I-beams (to obtain four-point bending). The test setup is presented in Fig. 3. Loading was applied monotonically in displacement control mode at a rate of 0.05 mm/sec. Loading was paused at every 10 kN intervals to mark the crack propagation and study the failure progression. All the specimen displacements were recorded using Linear Variable Displacement Transducers (LVDTs). LVDTs were positioned at specific locations (at mid span and at a distance of one third of the span from support) along the length of the beam to capture the entire curvature profile during testing. Strain gauges of 5 mm gauge length were instrumented on the prestressing strands at mid-span location to capture the strain variation during testing. Data acquisition system (DAQ) was used to acquire and store the data from external instrumentation.

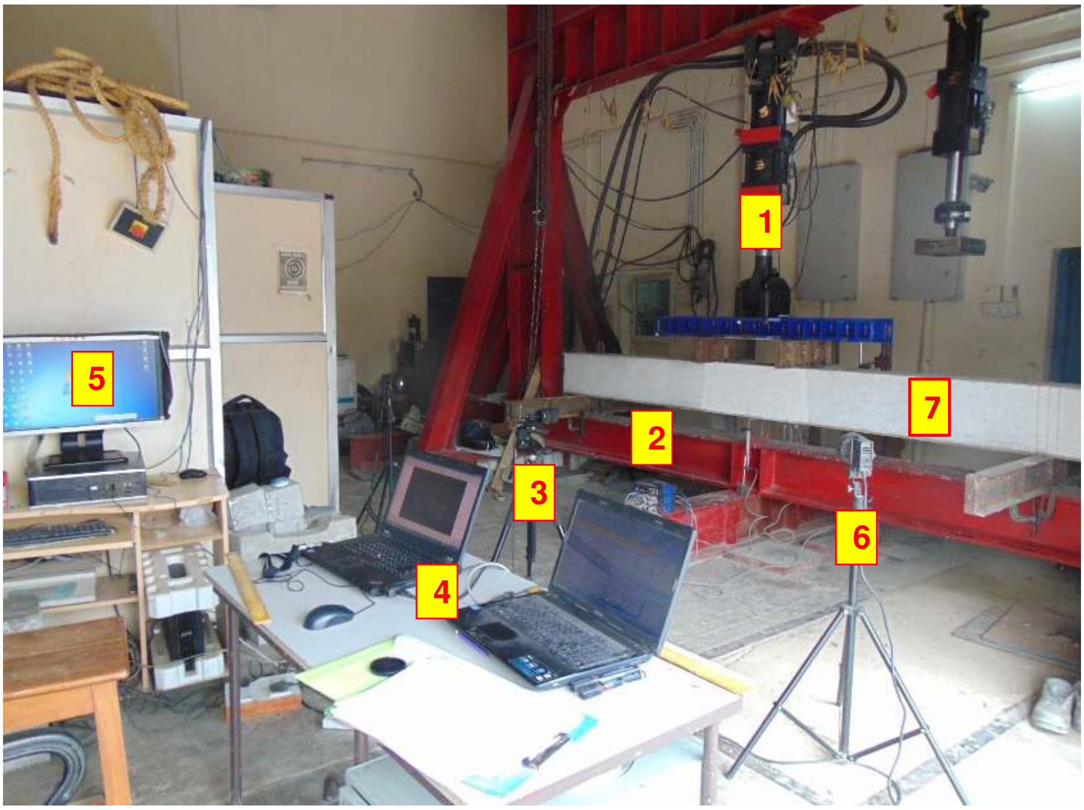

1. 250 kN MTS Actuator; 2.HBM DAQ system; 3.Camera; 4. DAQ Controller; 5. MTS Controls system; 6. Light source; 7. Test Specimen

Fig. 3: Test setup and Instrumentations

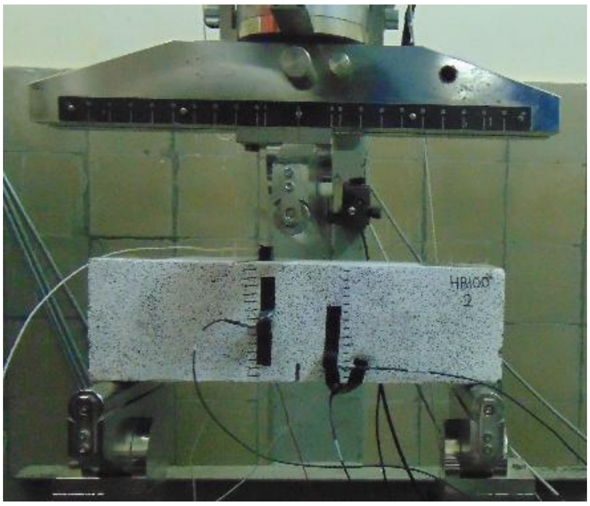

Fig. 4: Fracture test setup

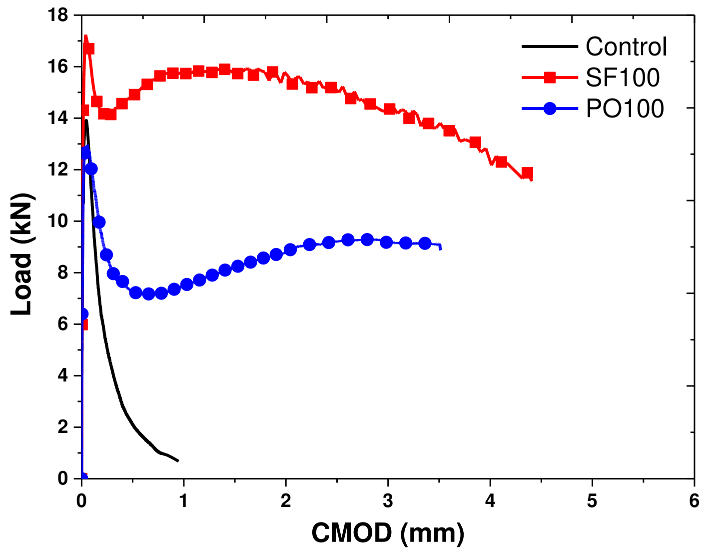

Fig. 5: Load-CMOD response of fiber reinforced specimen

4.0 TEST RESULTS AND DISCUSSION

4.1 Fracture behaviour of fiber reinforced concrete (FRC)

As part of a companion study, fracture tests were conducted on steel and polyolefin reinforced beam samples under flexure to understand the efficiency of steel and synthetic fibers with 1% volume fraction of fibers. The test setup and results are presented in Fig. 4, 5. Load vs crack mouth opening displacement (CMOD) response of fiber-reinforced specimens with steel (SF 100) and synthetic fibers (PO 100) is shown in Fig. 5. The load vs CMOD curves indicate that steel fiber restrict the crack opening more efficiently than that of macro-synthetic fiber at same fiber dosages. The load drop after the peak load is minimum in case of steel fiber reinforced specimen due higher elastic modulus and tensile strength of steel fiber.

4.2 Load-deflection behaviour

The load vs mid-span displacement of beams are compared in Fig. to understand the contribution of steel and polyolefin fiber towards the load resistance. The load displacement curves presented in Fig. depicts the behaviour of the specimens with particular dosage/type of fibers to that of the control specimen (without fibers). Details such as overall behaviour of beams in terms of cracking load, post cracking stiffness, peak load, displacement at failure and failure mode are summarized in Table 5. Though two specimens of SF100 series were cast, one of the specimens had honeycombing due to improper compaction and is discarded for further comparisons. In addition, one of the PO100 specimens had an instrumentation error and hence is not used for comparison of load-displacement curves. For the control specimens, the first crack appeared on the tension fibers near the loading point at a load of 60 kN (Table 6). After cracking, stiffness degradation was observed due to formation of multiple cracks. Finally, the specimen failed in flexure-shear mode at a peak load of 130 kN corresponding to a displacement of 52 mm. The strands just yielded before reaching peak load due to low reinforcement ratio used in the beams.

Fig. 6a shows the load displacement behaviour of beams with 0.35% fiber dosage. Both the beams with steel and polyolefin exhibited similar behaviour before cracking. Post-cracking stiffness increased in fiber-reinforced beams as compared to post cracking stiffness of control specimen. This increase in stiffness is mainly due to contribution of fibers in crack bridging. However, the steel fiber specimen exhibited stiffer post-cracking response than the specimen with synthetic (polyolefin) fibers. Both the control and synthetic fiber reinforced specimens (PO-35) cracked at 60 kN while the steel fiber reinforced specimen (SF35) cracked at 69 kN. The addition of steel fiber (0.35%) improved the cracking load and post-cracking stiffness by 15% and 36% respectively when compared to synthetic fibers (0.35%) (Fig. 6a). A peak load increment of 4.8% was observed in SF35 when compared to PO35. Post-peak behaviour was almost similar for both steel and synthetic fibers at 0.35% dosage. Steel fiber reinforced specimens (SF35) failed in flexure mode while the specimens reinforced with synthetic fibers (PO35) failed in flexure-shear mode. In this study, if the final failure of beam is due to shear tension cracking after the yielding of prestressing strand, it is defined as the flexure-shear mode.

The comparison of behaviour at 0.7% fiber dosage exhibited by SF70 and PO70 is depicted in Fig. 6b. In comparison to control specimen, due to the higher modulus of steel fibers, SF specimens exhibited a higher cracking load when compared to the PO specimens (Table 5). Average post-cracking stiffness of the SF70 was found to be 12% more than that of PO70 (Fig. 6b). Though diagonal shear cracks formed in both the SF and PO specimens (0.70%), the fibers were effective in arresting the propagation of shear cracks, which resulted in the formation of flexural cracks. Due to limitation in stroke capacity of the actuator, the test was terminated when the actuator displacement reached vicinity of 100 mm (for specimens SF70 and PO70). The average peak load for SF70 and PO70 was observed to be 147 kN and 140 kN, respectively. In case of beams with 1.0% fiber dosage, the cracking load of steel fiber specimen (SF100) was 70 kN (Fig. 6c). Soon-after cracking, in comparison to synthetic fibers, steel fibers contributed more efficiently to crack arresting. This is mainly due to higher modulus of elasticity of the steel fibers. The synthetic fiber specimen (PO100) reached a peak load of 135 kN. Presence of steel fibers of same volume improved the peak load by 17% and post-cracking stiffness by 46% when compared to the synthetic fiber reinforced specimen. The testing was terminated for SF100-2 and PO100-1 when the mid-span deflection reached 100 mm due to limitation in the stroke capacity of the actuator.

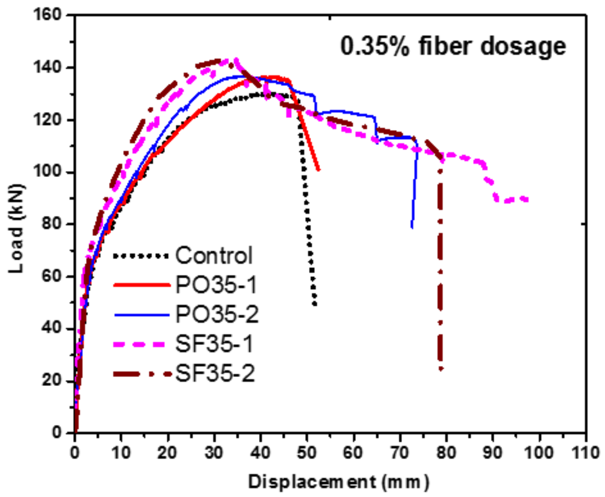

(a) Beams with 0.35% dosage of fibers

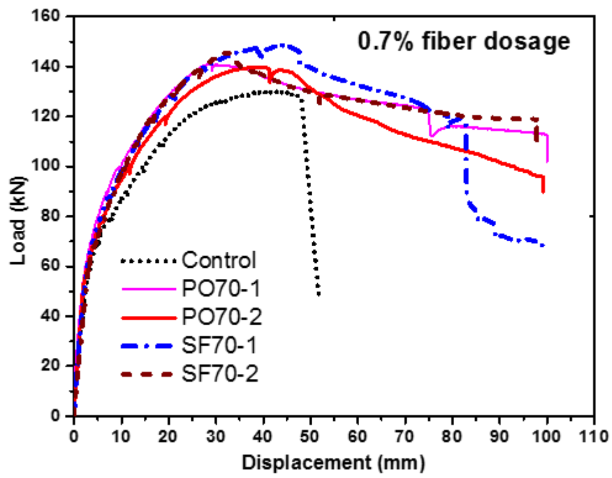

(b) Beams with 0.7% dosage of fibers

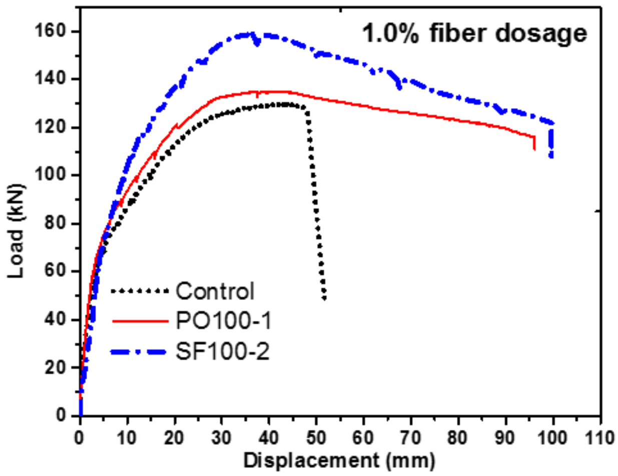

(c) Beams with 1.0% dosage of fibers

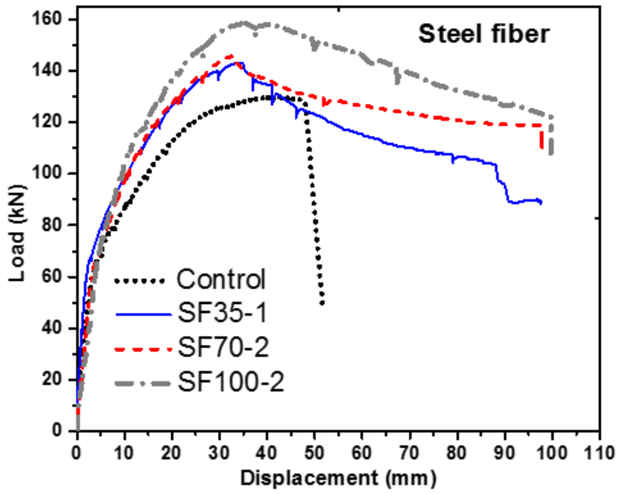

(d) Beams with Steel fibers

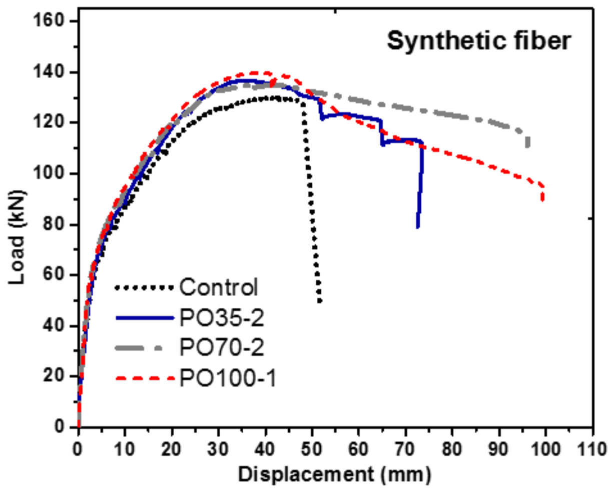

(e) Beams with synthetic fibers

Fig. 6: Comparison of Load-Deflection behaviour

The difference in the behaviour with steel and synthetic fibers can be clearly noticed at high fiber dosage of 1.0% (Fig. 6c). Steel fibers were more efficient in improving the serviceability performance. Fig. 6 (d, e) indicates the behaviour of PSC beams with steel and synthetic fibers separately. The experimentally observed cracking and peak moment was verified by RILEM 162-TDF[17] recommendations as shown in Table 5. RILEM 162-TDF[17] approach was used for both steel and synthetic fiber specimens by suitably modifying the tensile stress strain curves from literature [29,33]. More details on the RILEM calculations of fiber reinforced prestressed concrete beams can be found elsewhere [29, 33,34].

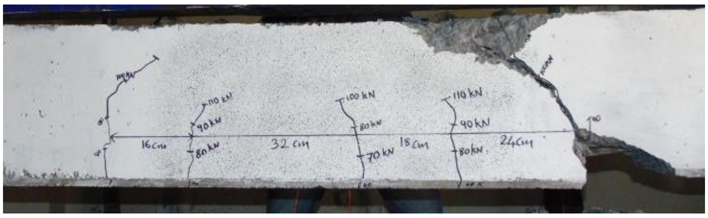

(a) Control Beam (Flexure-Shear Mode)

(b) SF35 (Flexure Mode)

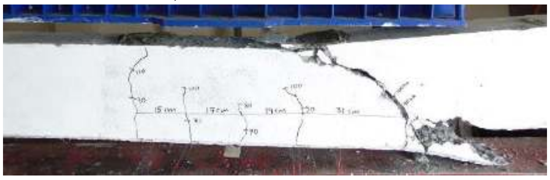

(c) PO35 (Flexure Shear Mode)

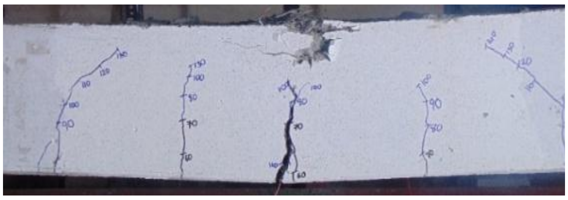

(d) SF70 (Flexure Mode)

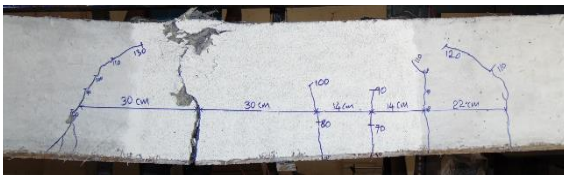

(e) PO70 (Flexure Mode)

(f) SF100 (Flexure Mode)

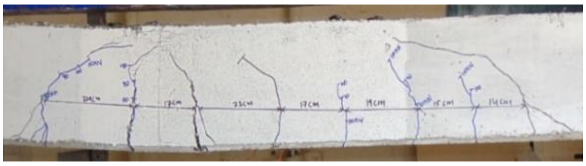

(g) PO100 (Flexure Mode)

Fig. 7: Failure modes of PSC beam with steel and synthetic fiber

4.3 Crack Distribution and Failure Modes

The crack distribution and failure modes of the tested specimens is detailed below. Crack propagation of different specimens at three levels of loading is presented in Table 6. Control beam had few flexural cracks between the loading points. At higher loads, the prestressing strands reached their yielding strain, on further increase in loads, flexural crack converted to shear and propagated through aggregates leading to sudden energy release at failure. The flexure-shear failure mode of control specimen is presented in Fig. 7a and Table 6. Beams with low dosage (0.35%) of fibers exhibited multiple flexure cracks and better crack distribution.

Steel fibers arrested the propagation of shear crack and changed the failure of specimens (SF35) to flexure dominant mode (Fig. 7b, Table 6). However, PO35 specimens still failed in flexure-shear mode (Fig. 7c) due to lesser efficiency of synthetic fibers in arresting the shear cracks.

In the specimens with moderate dosage (0.7%) of fibers, crack bridging effect of fibers was evident in steel specimens (SF70). Steel fiber reinforced specimens exhibited flexure dominant behaviour (Fig. 7d). In synthetic fiber reinforced specimen (PO70), the propagation of shear cracks was arrested and led to flexure dominant behaviour (Fig. 7e, Table 6). Both PO100 and SF100 specimen had numerous flexural cracks and experienced good amount of inelastic deformation. Addition of steel at high fiber dosage resulted in better distribution of flexural cracks and exhibited significant crack bridging (Fig. 7f,g). Addition of fibers improved the ductility as the fibers in the matrix formed a closed network, which hindered the formation of crack and its propagation. Even during the crack growth, the fibers in the matrix bridged the crack and prevented its further propagation. Thus, the presence of the fibers bridges the cracked surfaces and provides a restricting effect to the crack path. This increases the possibility of redistribution of stresses in the fracture process and improves the ductility of the specimen.

Table 5: Summary of test results

Parameters for Comparison	Control	SF35-1	SF35-2	PO35-1	PO35-2	SF70-1	SF70-2	PO70-1	PO70-2	SF100-2	PO100-1
	0.00%	0.35%				0.70%				1.00%	
Cracking load, P_{cr} (kN)	60	68	70	60	60	70	67	60	60	70	60
Deflection at Cracking load, Δ_{cr} (mm)	4.76	3.02	3.28	3.02	3.22	4.03	4.02	2.45	2.813	4.66	2.81
Peak load, P_{pl} (kN)	130.0	143.0	143.5	136.6	136.8	148.6	146	141.1	139.7	159	135.1
Increase in P_{pl} (%)	-	10.0	10.4	5.1	5.2	14.3	12.3	8.5	7.5	22.3	3.9
Deflection at peak load, Δ_{pl} (mm)	42.7	34.4	29.6	43.3	36.5	45.0	32.4	29.0	38.5	36.6	39.1
Mid-span deflection at failure (Δ_f) (mm)	51.7	97.5	78.8	52	73.5	99.0*	97.8*	99.9*	99.2*	99.7*	96.1*
Post cracking stiffness (kN/mm)	2.06	2.903	3.457	1.962	2.710	3.076	3.335	3.133	2.572	3.871	2.656
Increase in post cracking stiffness (%)	-	41.0	68.0	-	31.6	49.4	62.0	52.1	25.0	88.0	29.0
Strain Energy (Joule)	5481	9309	10989	5758	8464	11534	11774	12000	11291	13239	11453
% increase in strain energy	-	69.8	100.5	5.1	54.4	110.4	114.8	118.9	106.0	141.5	109.0
Peak load Ratio $\left(\frac{SF}{PO}\right)$		1.05				1.05				1.17	
Post cracking stiffness ratio $\left(\frac{SF}{PO}\right)$		1.36				1.12				1.46	
Cracking Moment(kN-m) (Experimental)	37.50	43.12		37.50		42.81		37.5		43.75	37.5
Peak Moment(kN-m) (Experimental)	81.25	89.53		85.43		92.06		87.75		99.37	84.43
Cracking Moment(kN-m) (RILEM 162-TDF)	32.00	34.60		38.92		37.00		37.75		39.50	36.68
Peak Moment(kN-m) (RILEM 162-TDF)	81.00	86.00		82.96		90.00		85.62		95.00	88.16

Note:

- SF and PO are specimens containing steel and polyolefin fibers, respectively
- * Test was terminated at 100 mm due to limitation in stroke capacity of the actuator.

Table 6: Crack Propagation at Different Load Levels

	Fiber dosage	at cracking	at 120kN	Final stage
Control Speciemen	**-**	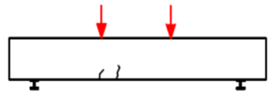	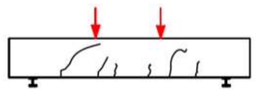	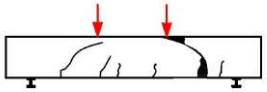 **Flexure Shear Mode**
SF35	**0.35%**	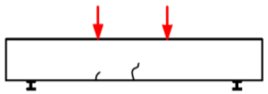	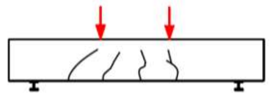	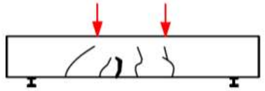 **Flexure Mode**
PO35		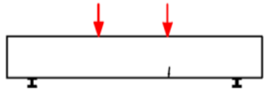	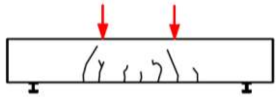	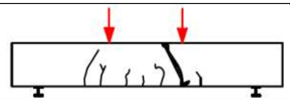 **Flexure-Shear Mode**
SF70	**0.7%**	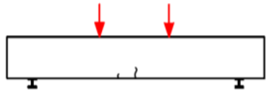	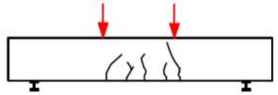	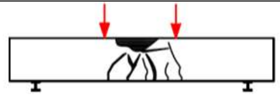 **Flexure Mode****
PO70		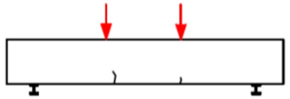	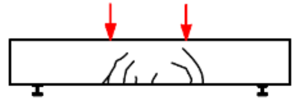	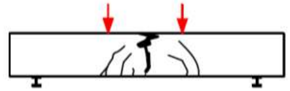 **Flexure Mode****
SF100	**1.0%**	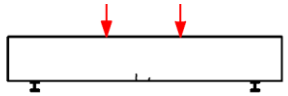	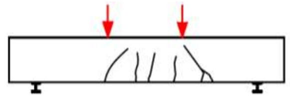	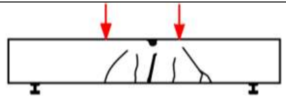 **Flexure Mode****
PO100		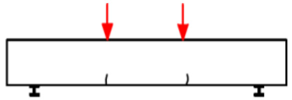	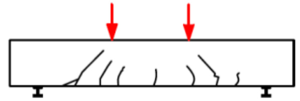	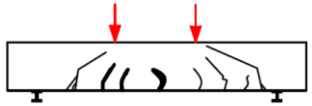 **Flexure Mode****

** Test was terminated due to limitation on actuator stroke capacity, but the specimens exhibited more of flexure dominant behaviour .

4.4 Load vs. Prestressing Strand Strain Behaviour

The strain in the prestressing strands was measured using strain gauges installed during the pre-tensioning process. Initial prestressing strain was measured to be 4000 μm/m. The applied prestressing force was released once the concrete attained a minimum compressive strength of 40 MPa. The initial loss in applied prestressing force was measured to be about 400 micro strain. The variation of strain with respect to the applied load was measured and presented in Fig. 8. As the prestressing strands do not possess a well-defined yield point, a value of 10,000 μm/m is considered as yield strain (ε_{py}) [35].

From the Fig.8, with the increase in steel fiber dosage, the reduction of strain in strands at same load level is noticeable. This reduction in strand strain can be attributed to the increase in effective contribution of fibers in arresting the propagation of cracks with the increase in steel fiber dosage. The same phenomenon was illustrated by synthetic PO fibers at lower dosage of fibers (0.35%, 0.7%). Additionally, it can also be observed from Fig. that at 0.35% and 0.70%, both SF and PO specimens exhibited similar strain variations in prestressing strand.

At higher steel fiber dosage of 1.0%, the strain in strand reduced significantly at same load level when compared to the control specimen. In all the specimens, the strands reached their yield strain because of low reinforcement ratio of the specimens. Due to malfunctioning of the strain gauges, the complete load strain curves could not be presented in the graphs. The yielding strain of the steel strand (10,000 micro strain) was reached in all the specimens before final failure (Fig. 8).

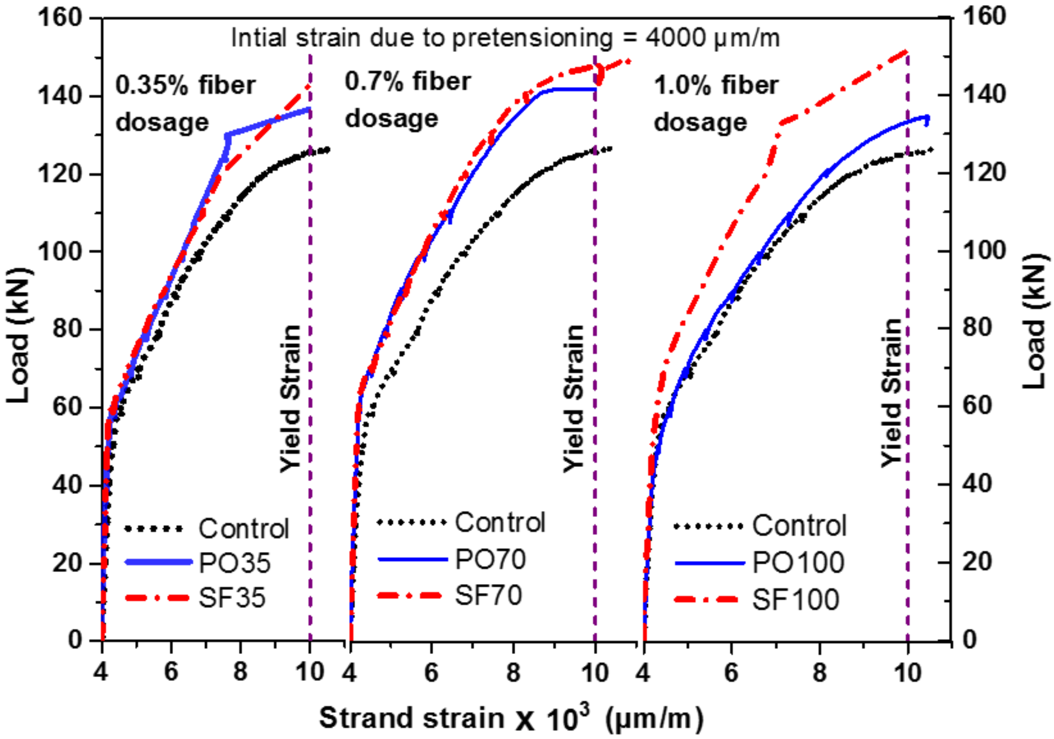

Fig. 8: Effect of Steel Fibers on Strain Variation of Strands in PSC Beams

4.5 Strain Energy Absorption capacity

Strain energy absorption capacity is one of the key factors in deciding the effectiveness of different fibers and its dosage for specific application. Strain energy absorption of the test specimens is calculated from the area under load-displacement curve until maximum displacement upto failure. Addition of fibers delays the crack propagation by bridging the cracked surfaces. Therefore, the specimen with higher fiber dosage had high energy absorption before failure. The energy absorption is closely related to the size of fracture process zone (FPZ). In FRC, FPZ covers a region of crack band and only the region along the crack path is affected by the cracking. Due to well-distributed cracks in flexure, the energy absorption increased significantly due to fiber addition. The energy absorption of steel and synthetic fibers is compared in Fig. 9. In general, the steel fiber specimens absorbed more strain energy when compared to macro synthetic fiber reinforced beams.

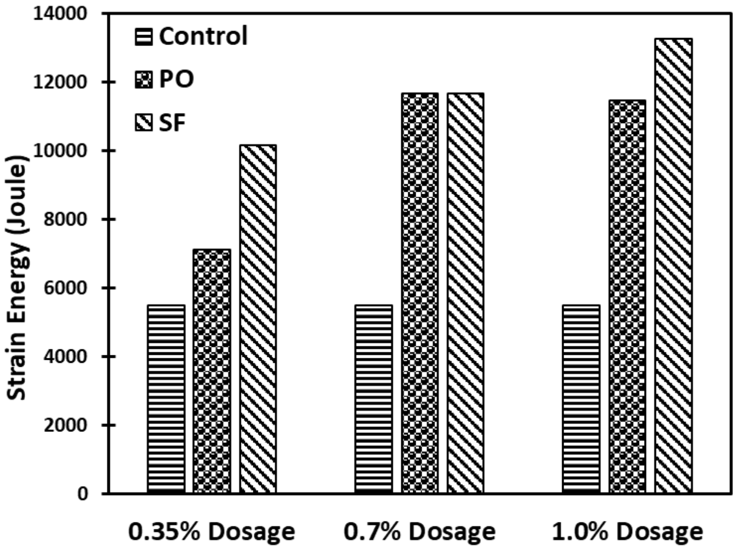

Fig. 9: Variation in strain energy absorption due to fiber addition

5 SUMMARY AND CONCLUSIONS

Prestressed concrete beams reinforced with steel and synthetic fibers were tested at a shear span to depth ratio of five to understand the efficiency of fibers in performance improvement. Based on the test results presented in this study, the following major conclusions can be drawn:

i) Both the steel and synthetic fibers improved the post-cracking behaviour and ductility of the prestressed concrete beams under flexure-shear.

ii) Steel fibers were more efficient in improving the post-cracking and ductility of the prestressed concrete beams at all fiber dosages.

iii) Addition of fibers helped in converting the less ductile flexure-shear mode to more ductile flexure mode. At low dosage (0.35%), only steel fibers were effective in arresting the shear cracks and ensured flexure dominant behaviour. However, the beams with high fiber dosage (0.70% and 1.0%) of steel as well as structural synthetic fibers ensured ductile flexural failure mode.

iv) Macro-synthetic fibers marginally increased the peak strength. However, steel fibers increased the peak strength significantly when compared to macro-synthetic fibers. The ultimate strength increased by 17% due to steel fibers when compared to synthetic fibers at 1.0% addition.

v) Energy absorption capacity of prestressed concrete beams increased with increase in both steel and macro synthetic fiber dosage. At all fiber dosages, steel fibers had higher energy absorption when compared to macro synthetic fibers.

ACKNOWLEDGEMENT

This experimental work was carried out as part of the project funded through Utchattar Avishkar Yojana (UAY) Scheme of Indian Government. PRECA India Pvt. Ltd. and Grenix India Ltd., sponsored the materials required for this research. Specimens were cast at casting yard of PRECA Ltd. The authors thankfully acknowledge the generous support of all the sponsors.

REFERENCES

1. ACI Committee 544, State of the Art Report on Fiber Reinforced Concrete, Michigan: ACI, Farmington Hills, 2002.
2. Tadepalli PR, Mo YL, Hsu TTC. Mechanical properties of steel fibre concrete, Mag. Concr. Res. 65 (8) (2013), 462-74.
3. Rasheed MA, Prakash SS. Mechanical behavior of sustainable hybrid-synthetic fiber reinforced cellular light weight concrete for structural applications of masonry, Constr. Build. Mater. 98 (2015), 631-40.
4. Jain S, Prakash SS, Subramaniam KVL. Monitoring of Concrete Cylinders with and Without Steel Fibers Under Compression Using Piezo-Ceramic Smart Aggregates, J. Nondes. Eval. 35 (4) (2016),59.
5. Srikar G, Anand G, Prakash SS. A study on residual compression behavior of structural fiber reinforced concrete exposed to moderate temperature using digital image correlation, Int. J. Con. Struct. Mat. 10 (1) (2016), 75-85.
6. Soetens T, Matthys S, Hertelé S, De Waele W. Shear behaviour of prestressed precast SFRC girders. Eng Struct (2017), 142, 20-35.
7. Yoo DY, Yuan T, Yang JM, Yoon YS. Feasibility of replacing minimum shear reinforcement with steel fibers for sustainable high-strength concrete beams. Eng Struct, 147(2017), 207-222.
8. Deng Z and Li J. Mechanical behaviors of concrete combined with steel and synthetic macro-fibers, Inter. J. of Physical Sciences Vol. 1 (2), pp. 057-066, October, 2006

9. Conforti A, Minelli F, Tinini A, Plizzari GA. Influence of polypropylene fibre reinforcement and width-to-effective depth ratio in wide-shallow beams. Eng Struct, 88 (2015), 12-21

10. Sahoo DR, Kumar N. Monotonic behavior of large-scale SFRC beams without stirrups. Eng Struct, 92 (2015), 46-54

11. Cuenca E, Serna P. Shear behavior of prestressed precast beams made of self-compacting fiber reinforced concrete, Constr. Build. Mater. J. 45 (2013), 145-56.

12. Tadepalli PR, Dhonde HB, Mo YL, Hsu TTC. Shear strength of prestressed steel fiber concrete I-beams, Int. J. Con. Struct. Mat. 9 (3) (2015), 267-81.

13. Dhonde HB, Mo YL, Hsu TTC, Vogel J. Fresh and hardened properties of self-consolidating fiber reinforced concrete ACI Mater. J. 104 (5) (2007), 491-500.

14. Conforti A, Minelli F, Plizzari GA. Shear behaviour of prestressed double tees in self-compacting polypropylene fibre reinforced concrete. Eng Struct, 146 (2017), 93-104.

15. Narayanan R, Darwish IYS. Shear in prestressed concrete beams containing steel fibres Int. J. Cem. Compos. Lightweight Conc. 9 (2) (1987), 81-90.

16. Yazdanbakhsh A, Altoubat S, Rieder KA. Analytical study on shear strength of macro synthetic fiber reinforced concrete beams. Eng Struct, 100 (1) (2015), 622-632.

17. T.C. Rilem162-TDF; Test and design methods for steel fibre reinforced concrete, σ-ε-design method. (Chairlady L. Vandewalle) Mater Struct, 36 (2003), 560-567.

18. FIB-Fédération Internationale du Béton. Model Code 2010 (first complete draft), bulletin 55, vol. 1(5) “Materials”. Lausanne 2010.

19. Alhozaimy AM, Soroushian P, Mirza F. Mechanical properties of polypropylene fiber reinforced concrete and the effects of pozzolanic materials, Cem. Concr. Compos. 18 (2) (1996), 85-92.

20. Thomas J, Ramaswamy A. Crack width in partially prestressed T-beams having steel fibers, ACI Struct. J. 103 (4) (2006), 568-76.

21. Harajli MH. Bond behavior in steel fiber-reinforced concrete zones under static and cyclic loading: experimental evaluations and analytical modeling, J. Mater. Civil Eng. 22 (7) (2010), 674-86.

22. Sahoo DR, Sharma A. Effect of steel fiber content on behavior of concrete beams with and without stirrups, ACI Struct. J. 111 (5) (2014), 1157-66.

23. Tiberti G, Minelli F, Plizzari GA, Vecchio FJ. Influence of concrete strength on crack development in SFRC members, Cem. Concr. Compos. 45 (2014), 176-85.

24. Ramzi BAA, Omer QA. Flexural strength of reinforced concrete T-Beams with steel fibers, Cem. Concr. Compos. 21 (2) (1999), 263-268

25. Abbas MY, Khan MI. Fiber-Matrix Interfacial Behavior of Hooked-End Steel Fiber-Reinforced Concrete, J. Mater. Civ. Eng. 28 (11) (2016), 04016115,1-10.

26. Yoo DY, Yoon YS, Banthia N. Flexural response of steel-fiber-reinforced concrete beams: effects of strength, fiber content, and strain-rate Cem. Concr. Compos., 64 (2015),84-92

27. Banthia N, Sappakittipakorn M. Toughness enhancement in steel fiber reinforced concrete through fiber hybridization, J Cem Concr Res, 37 (9) (2007),1366-1372

28. Fantilli AP, Mihashi H, Vallini P. Post-peak behaviour of cement-based materials in compression, ACI Mater J, 104 (5) (2007),501-510

29. Amin A, Foster SJ, Gilbert RI, Material characterisation of macro synthetic fibre reinforced concrete, Cement and Concrete Composites 84 (2017),124-133

30. IS 1343, Code of Practices for Prestressed Concrete, Bureau of Indian Standards, New Delhi, India, 1980.

31. IS 10262, Proportioning-Guideline, Indian Standard Concrete Mix, Bureau of Indian Standards, New Delhi, India, 2009.

32. Kani GNJ. How Safe Are Our Large Concrete Beams? ACI Struct. J. 64 (3) (1967), 128-41.

33. Neocleous K, Tlemat H, Pilakoutas K. Design issues for concrete reinforced with steel fibers, including fibers recovered from used tires. J Mater Civ Eng, 18 (2006), 677-685.

34. Joshi S, Thammishetti N, Prakash SS, Jain S. Cracking and ductility analysis of steel fiber reinforced prestressed concrete beams in flexure, ACI Structural Journal (2018) (Accepted).

35. Devalapura RK, Tadros MK. Stress-strain modeling of 270 ksi low-relaxation prestressing strands, PCI J. 37 (2) (1992), 100-105.